

## 1 **Biochemical Barriers on the Path to Ocean Anoxia?**

2 Stephen Giovannoni<sup>a\*</sup>, Francis Chan<sup>b\*</sup>, Edward Davis<sup>c</sup>, Curtis Deutsch<sup>d</sup> and Sarah Wolf<sup>a</sup>

3 \*The first and second authors shared equally in developing this manuscript

4 <sup>a</sup>#Department of Microbiology, Oregon State University, Corvallis, OR, USA

5 <sup>b</sup>Department of Integrative Biology, Oregon State University, Corvallis, OR, USA

6 <sup>c</sup>Center for Genome Research and Biocomputing, Oregon State University, Corvallis, OR, USA

7 <sup>d</sup>University of Washington, School of Oceanography, Seattle, WA, USA

8 Running title: Hypoxic Barrier Hypothesis

9 Word count: 3,265

10 Mailing address: Department of Microbiology, Oregon State University, 220 Nash Hall,

11 Corvallis, OR 97331; Phone: (541) 737-1835; Fax: (541) 737-0496.

12 mBio: Opinions/Hypotheses

13 Corresponding author: [steve.giovannoni@oregonstate.edu](mailto:steve.giovannoni@oregonstate.edu)

### 14 **ABSTRACT (154/250 words)**

15 The kinetics of microbial respiration suggest that, if excess organic matter is present, oxygen  
16 should fall to nanomolar levels, in the range of the Michaelis-Menten constants ( $K_m$ ). Yet even in  
17 many biologically productive coastal regions, lowest observed  $O_2$  concentrations often remain  
18 several orders of magnitude higher than respiratory  $K_m$  values. We propose the *Hypoxic Barrier*  
19 *Hypothesis* (HBH) to explain this apparent discrepancy. The HBH postulates that oxidative  
20 enzymes involved in organic matter catabolism are kinetically limited by  $O_2$  at concentrations far  
21 higher than the thresholds for respiration. We found support for the HBH in a meta-analysis of  
22 1137  $O_2$   $K_m$  values reported in the literature: the median value for terminal respiratory oxidases  
23 was 350 nM, but for other oxidase types the median value was 67  $\mu$ M. The HBH directs our

24 attention to the kinetic properties of an important class of oxygen-dependent reactions that could  
25 help explain the trajectories of ocean ecosystems experiencing O<sub>2</sub> stress.

## 26 **IMPORTANCE (87/150 words)**

27 Declining ocean oxygen associated with global warming and climate change is impacting marine  
28 ecosystems across scales from microscopic planktonic communities to global fisheries. We  
29 report a fundamental dichotomy in the affinity of enzymes for oxygen. The importance of this  
30 observation has yet to be fully assessed, but it is predicted to impact the rate at which organic  
31 matter is oxidized in hypoxic ecosystems, and the types of organic matter that accumulate.  
32 Competition between intracellular enzymes for oxygen may also have impacted microbial  
33 strategies of adaptation to suboxia.

## 34 **KEYWORDS**

35 oxygen minimum zones, oxygenase K<sub>m</sub>, ocean respiration, dissolved organic matter

## 36 **INTRODUCTION**

37 Marine suboxic and anoxic zones are hotspots of microbially-mediated biogeochemical  
38 transformations that regulate the nitrogen budget and air-sea fluxes of greenhouse gases of the  
39 global ocean (1). Because dissolved oxygen (DO) also organizes the structure and dynamics of  
40 ocean food webs, understanding the processes that regulate expansion of suboxic and anoxic  
41 zones in response to past and current climate changes is a pressing challenge (2). Suboxic and  
42 anoxic zones are embedded within broader oxygen minimum zones (OMZ) that comprise some  
43 8% of the surface area of the ocean. While recent advances in nanomolar-scale DO measurement  
44 technologies have enabled precise delineation of the presence of suboxia and anoxia (3), we

45 contend that a perplexing yet fundamental question has been overlooked. Given our canonical  
46 understanding of microbial respiration kinetics, why are suboxia and anoxia not a much more  
47 pervasive feature of the ocean's low oxygen zones?

48 Of biological reactions that consume O<sub>2</sub>, by far the most important, in terms of mass, is carbon  
49 respiration. Michaelis-Menten half saturation (K<sub>m</sub>) constants for respiration are typically very  
50 low, on the order of a few nanomolar, although higher values have been reported (4) (**Figure 1**).  
51 Thus, if labile organic carbon, i.e. compounds that readily can be used as a source of electrons  
52 for respiration, is delivered in excess to a microbial ecosystem, DO declines at a rate determined  
53 by the respiratory capacity of the microorganisms present and the supply of organic matter.  
54 Importantly, the minimum DO attainable should reflect the well-described high-affinity,  
55 nanomolar scale K<sub>m</sub> of microbial respiratory oxidases (5). Other factors that can influence DO in  
56 aquatic ecosystems include: photosynthesis, when light is present; oxygen transport by ocean  
57 currents and mixing; diffusion, which can limit respiration, particularly in aggregates of cells;  
58 impacts of low oxygen on grazing metazoa (6), which require higher oxygen concentrations than  
59 bacteria; non-respiratory biochemical reactions that consume oxygen; and abiotic reactions that  
60 consume oxygen (7). Nonetheless, DOM formation and oxidation is the mechanistic centerpiece  
61 in our fundamental understanding of microbial-scale processes leading to low oxygen states and  
62 predictions of global ocean oxygen dynamics.

63 Eastern boundary upwelling systems (EBUS) represents one of the ocean's most productive  
64 biomes. In these coastal ecosystems, oxygen-poor subsurface waters uplifted from the vertical  
65 periphery or core of open ocean OMZs receive elevated organic carbon inputs from surface  
66 phytoplankton blooms. **Figure 2** shows relative water volumes for DO concentrations across  
67 these systems. Of the ocean's four major EBUS, only the Peru-Chile Current System in the

68 Eastern Tropical Pacific Ocean persistently exhibits DO-deficient states in continental shelf  
69 waters. For both Pacific EBUS, there is an accumulation of water volumes below 100  $\mu\text{M}$  but a  
70 sharp drop-off in volume of waters that reach suboxic ( $<5 \mu\text{M}$ ) or anoxic ( $\sim 0 \mu\text{M}$ ) states in the  
71 upper ocean (0-400 m) including continental shelf waters where remineralization and oxygen  
72 loss is most active (Fig 2b). The pattern is striking - despite the nanomolar-scale of respiratory  
73  $K_m$  values, respiration in productive EBUS is able to draw down DO to hypoxic levels but rarely  
74 is able to consume the last 10-60  $\mu\text{M}$  DO. While the depth of OMZs extends below 400 m, the  
75 failure of suboxic and anoxic volumes to accumulate despite the presence of large volumes of  
76 hypoxic water persists when we expand our sampling to 1000 m (Fig 2d).

77 To explain the observations in **Figure 2**, we propose the *Hypoxic Barrier Hypothesis (HBH)*,  
78 **which states: dissolved  $\text{O}_2$  kinetically limits the activity of oxygenase enzymes involved in the**  
79 ***breakdown of organic matter, in the range of oxygenase  $K_m$  values (median value 67  $\mu\text{M}$ )***  
80 ***causing a decline in DOM oxidation rates in ecosystems experiencing oxygen stress, and an***  
81 ***accumulation of DOM that is catabolized by pathways that require oxygenases.*** The HBH  
82 ascribes the decline in  $\text{O}_2$  frequency distributions of suboxic and anoxic waters (Figures 2 and  
83 S2) to fundamental biochemical properties of cells, particularly the mechanisms by which  
84 oxidative enzymes cleave semi-labile organic matter, making it accessible to further oxidation.

85 **Oxygen depletion by respiration in aquatic systems.** How far can respiring marine bacteria  
86 lower oxygen concentrations when they are provided with an ample supply of reductant for  
87 respiration, as would be expected for plankton in the presence of an excess of labile organic  
88 carbon? The Pasteur Point is an influential concept based on the observation that facultative  
89 anaerobes switch to fermentation at ca. 2.2  $\mu\text{M}$   $\text{O}_2$ , approximately an order of magnitude below  
90 the average  $K_m$  for oxygenases (Fig 1), steep declines in suboxic and anoxic water volumes in

91 EBUS (Fig 2), and the ca. 25  $\mu\text{M}$  inflection in cumulative frequency distribution of DO  
92 observations recorded in CCS (Fig. S2). Newer information suggests that the limits of bacterial  
93 respiration are in the nanomolar range. This is consistent with the observation of high affinity  
94 cytochromes that exhibit  $\text{O}_2$   $K_m$  between 3 and 200 nM (8; Figure 1). Higher  $\text{O}_2$  Michaelis  
95 constants have been sometimes been reported for marine bacteria, but it has been suggested that  
96 higher values obtained with whole cells reflect diffusion limitation, which can be expected to  
97 inflate apparent  $\text{O}_2$  Michaelis constants in proportion to cell sizes and respiration rates. Stolper et  
98 al. showed that *E. coli* cells could grow at less than 3 nM  $\text{O}_2$ , a sufficiently low concentration to  
99 limit growth by diffusion, but high enough to sustain growth through  $\text{O}_2$  respiration (8). Our  
100 meta-analysis of indicates that cells grown on highly labile carbon compounds such as glucose  
101 display whole cell  $\text{O}_2$   $K_m$  values extends well into nanomolar  $\text{O}_2$  concentrations. We conclude  
102 that a substantial background of observations and theory support the conclusion that the  
103 respiration rate of chemoheterotrophic cells should not be limited by  $\text{O}_2$  at concentrations found  
104 in ocean hypoxic zones or the Pasteur Point at ca. 2.2  $\mu\text{M}$ .

105 The accumulation of hypoxic and scarcity of suboxic or anoxic volumes in the ocean nonetheless  
106 suggest that negative feedbacks between oxygen decline and respiration may be at play. Direct  
107 measurements of microbial  $\text{O}_2$   $K_m$  in natural systems are rare but available evidence point to  $K_m$   
108 values far higher than the nanomolar values reported from laboratory cultures with labile carbon  
109 sources. Working in the Arabian Sea OMZ, Keil et al. (9) observed an apparent  $K_m$  of 20  $\mu\text{M}$   $\text{O}_2$   
110 for microbial community respiration. In the Nambian and Peruvian OMZ, Kalvelage et al. (10),  
111 reported a linear decline in respiration rate between 20 and 0  $\mu\text{M}$   $\text{O}_2$ . In Chesapeake Bay, a  
112 hypoxia-prone system, microbial respiration rates saturate at  $[\text{O}_2]$  above 25  $\mu\text{M}$  (11), a pattern  
113 that we have similarly found for the CCS OMZ (Figure S3). Holtappels et al. (12) further

114 reported linear declines in respiration rates between 14 and 1  $\mu\text{M}$   $\text{O}_2$  in waters collected from a  
115 fjord in Denmark. These results are surprising because researchers using the same methods have  
116 also found many instances of nM  $K_m$  values for microbial respiration. This suggests a bimodal  
117 distribution of  $\text{O}_2$   $K_m$  values that differ by upwards of three orders of magnitude. Telescoping out  
118 further, global models of ocean  $\text{O}_2$  and carbon export converge on  $K_m$  values of between 4 and  
119 20  $\mu\text{M}$   $\text{O}_2$  in order to optimize fit between model and observations (13, 14). What accounts for  
120 the disparity between accumulation of hypoxic water volumes, the  $\mu\text{M}$  scale  $K_m$ 's reported from  
121 natural systems and used to fit models, and nM scale  $K_m$ 's predicted by respiratory oxidases?  
122 Biochemistry offers a mechanistic explanation for this apparent disparity. There is evidence in  
123 the scientific literature suggesting that microbial respiration of some types of organic matter is  
124 slows when oxygen concentrations fall low enough to inhibit catabolic oxygenase enzymes.  
125 Kroonman et al. (15), studying 3-chlorobenzoate degradation by the bacterium *Alcaligenes*,  
126 reported two  $K_m$  values for  $\text{O}_2$  uptake. They attributed the lower value (65 nM) to respiration  
127 and the higher value (7-17  $\mu\text{M}$ ) to the activity of dioxygenases. Leahy and Olsen (16), studying  
128 toluene degradation by *Pseudomonads*, also reported biphasic kinetics for toluene catabolism as  
129 a function of oxygen concentration. The slope of the oxygen response declined with an inflection  
130 at 20 - 30  $\mu\text{M}$   $\text{O}_2$ . In both of these cases the behavior of the cultured cells oxidizing recalcitrant  
131 compounds is remarkably similar to the generalized behavior of ocean ecosystems approaching  
132 hypoxia.

133 To further explore the distribution of  $\text{O}_2$   $K_m$  values among biological reactions, we conducted a  
134 metanalysis of published data, shown in **Figure 1; Figure S1A; Table S1**. For  $\text{O}_2$   $K_m$  values  
135 reported in the literature, the median value for terminal respiratory oxidases was 350 nM, but for  
136 other oxidase types the median value was 67  $\mu\text{M}$ . The difference of ~100 fold in median values

137 was supported by a p-value of  $<2e-16$  in a t-test of the linear mixed-effect model coefficient  
138 comparing the log-transformed  $O_2$   $K_m$  values (17). The bimodal distribution of  $O_2$   $K_m$  observed  
139 at the enzyme scale is also repeated in whole cell studies. Cells that are grown on more complex  
140 organic carbon sources have a median respiratory  $K_m$  value of 20  $\mu M$ , while cells grown on  
141 highly labile organic carbon such as glucose have median  $K_m$  of 690 nM (Figure S1B).

142 Many enzymes that catalyze the biological breakdown of organic matter use oxygen as a  
143 substrate, yielding partially oxidized products that are metabolized further through catabolic  
144 pathways. These enzymes are often classified as either monooxygenases (mixed function  
145 oxidases) or dioxygenases. Enzymes in both families evolved to use  $O_2$  as a substrate, but  
146 monooxygenases incorporate a single oxygen atom into the substrate, reducing the second atom  
147 to water, whereas dioxygenases typically add both atoms of the reacting  $O_2$  to the product. A  
148 geochemically important example of a monooxygenase is the heme-dependent Mn peroxidase  
149 that catalyzes oxidation of lignin, a phenolic oligomer. Fungal ligninases belong in the heme-  
150 dependent peroxidase superfamily (18). Ligninases evolved in the Paleozoic, and it has been  
151 postulated that their origin resulted in widespread biodegradation of wood, causing the end of the  
152 carboniferous period, and rises in global atmospheric  $CO_2$  (19). Another superfamily of oxidases,  
153 the flavin-dependent monooxygenases, are among the most diverse and prevalent proteins known.  
154 They catalyze a wide range of reactions, for example hydroxylation, Baeyer–Villiger oxidation,  
155 oxidative decarboxylation, epoxidation, desulfurization, sulfoxidation and oxidative denitration  
156 (20). Many of the reactions catalyzed by flavin-dependent monooxygenases initiate the  
157 catabolism of compounds that are otherwise recalcitrant to oxidation. These enzymes share a  
158 common mechanism in which reduced flavin reacts with oxygen to produce a flavin C4a-  
159 (hydro)peroxide that then reacts with electrophilic or nucleophilic substrates, typically resulting

160 in the consumption of one diatomic oxygen molecule, the addition of an oxygen atom to the  
161 substrate, and the release of water. Also important are the dioxygenases, which belong to a  
162 different protein family also feature prominently in DOM degradation particularly for aromatic  
163 compounds. These protein families came to the attention of oceanographers recently when it was  
164 discovered that cells of one of the important oceanic bacterial clades, SAR202, harbor expanded  
165 clusters of paralogous genes from both of these protein types (21). It has been proposed that  
166 these enzymes participate in the oxidation of semi-labile organic matter, initiating its breakdown.

167 The meta-analysis of  $O_2$   $K_m$  values presented in Figure 1 suggests that micromolar  $DO$  sensitivity  
168 is ubiquitous across metabolic processes. Among the "other oxidase" types, we observed no clear  
169 trends that associated  $O_2$   $K_m$  values with protein families sorted by COGs or other precise  
170 functional groups, such as enzyme commission classifications. In contrast, cytochrome  
171 respiratory proteins with heme cofactors consistently displayed a much higher affinity for  
172 oxygen than other protein types. Phylogenetically, the distribution of  $O_2$   $K_m$  values included  
173 diverse bacteria, including Proteobacteria, Actinobacteria, Firmicutes, and Cyanobacteria, as  
174 well as eukaryotic organisms including fungi, humans, and other chordates.  $O_2$   $K_m$  values showed  
175 a 100-fold difference between respiratory and non-respiratory oxidases regardless of taxonomic  
176 group. We conclude that this pattern is robust to phylogenetic bias in  $O_2$   $K_m$  value sampling.  
177 While our focus in the current work is marine systems, the HBH in principle applies to all  
178 ecosystems.

179 **The role of oxidases in organic matter degradation.** Oceanographers classify organic matter  
180 by its half-life, frequently using the category "labile dissolved organic matter" (LDOM) to  
181 describe dissolved organic matter that is oxidized in minutes to hours, or at most a few days,  
182 while the term "semi-labile" (SLDOM), and sometime "recalcitrant" are used to refer to



183 dissolved organic matter that persists longer, but is eventually oxidized. Here we introduce a new  
184 term, "oxygen-dependent DOM" (ODDOM) to describe DOM that is catabolized via reactions  
185 that require the activity of oxygenases and thus are susceptible to inhibition when O<sub>2</sub>  
186 concentrations reach values in the range of ca. 10-100 μM. We'll confine the discussion to  
187 dissolved forms of organic matter, although most organic matter enters ecosystems as particulate  
188 organic matter (POM) and is subsequently converted to DOM before being used by  
189 microorganisms. Implicit in the above categories is the idea that different kinds of organic  
190 matter are accessible to biological oxidation through different mechanisms and at different rates.  
191 The HBH is consistent with the distribution of ocean anoxic zones if one assumes organic  
192 matters supplies are uneven. If LDOM is oversupplied relative to oxygen, for example by high  
193 rates of export production in systems with restricted circulation, then the activities of respiratory  
194 terminal cytochrome complexes would be expected to readily draw down DO to nM  
195 concentrations in accordance with their nM K<sub>m</sub> values. In natural systems, LDOM are rapidly  
196 depleted. As hypothesized, the activities of non-respiratory oxidases limit the supply of reductant  
197 to respiratory oxidases. This acts as a bottleneck that slows the rate of respiration as DO declines.  
198 With sufficient time, DO should reach minimum values as expected from nM K<sub>m</sub> values of  
199 respiratory oxidases. Such conditions can be met in the core of OMZs that have been isolated  
200 from the atmosphere over decadal to century time scales, and evidence of this can be seen in Fig.  
201 2.

202 The large disparity in K<sub>m</sub>'s we report between respiratory oxygenases and other oxygenase types  
203 has implications for microbial cell evolution and metabolic regulation at the cellular level.  
204 Inside of cells respiratory oxygenases could outcompete other oxygenases, exacerbating the  
205 slowing of some oxygen-dependent cellular processes at low oxygen. To avoid this, cells may

206 have evolved metabolic regulation that avoids such competitive interactions, for example by  
207 shifting to alternate electron acceptors before O<sub>2</sub> is depleted (22). This topic, which needs  
208 exploration, could help us understand how microbial cells have adapted to suboxic environments,  
209 which are far more common in the ocean than anoxic environments.

210 **Testing the HBH.** The HBH sets forth a number of central predictions that are testable by  
211 experimentation, observation, and modeling. The impact of biphasic oxygen dependence  
212 predicted by the HBH should be manifested as a broad potential for oxygen to limit microbial  
213 respiration across hypoxic systems in the range of oxygenase K<sub>m</sub> values (median value 67 μM),  
214 when LDOM is depleted, but not if excess LDOM is present. To test that prediction, we  
215 measured rates of respiration (oxygen uptake) in water samples from the Northern California  
216 Current System OMZ, where DO minimum reach only ~5 μM, well above canonical nM K<sub>m</sub> for  
217 cytochrome oxidases. DO was increased by the simple expedient of allowing air to be  
218 momentarily entrained during filling (**Figure S3**). In our experiments, and other similar  
219 experiments we found among published work, the addition of DO caused respiration rates to rise  
220 relative to controls. This observation could be attributed to the limitation of respiration by  
221 diffusion (20), but alternatively, it could result from mechanisms described in the HBH model  
222 we propose.

223 There are many other experimental avenues to testing the HBH that have not been explored.  
224 **Figure S2** scratches the surface of what could done with field experiments and mesocosms to  
225 verify predictions of the HBH. For example, experiments that test the biological availability of  
226 DOM at high (e.g. 200 μM) and moderate (e.g. 20 μM) DO could challenge these ideas.  
227 Mechanisms invoked by the HBH would lead to changes in the chemical composition of DOM  
228 as DO declines: the ratio of LDOM to ODDOM should decrease as DO approaches the K<sub>m</sub>

229 values of catabolic oxygenase enzymes for O<sub>2</sub>. Measurements of DOM chemistry could  
230 determine whether these changes occur as predicted. ODDOM, a term coined herein to segregate  
231 DOM into categories by chemical composition and oxygenase involvement in catabolism, is at  
232 present a theoretical concept, albeit grounded in the fundamentals of biochemistry. Although  
233 chemical oceanographers do not at present measure ODDOM, in principle methods such as high  
234 resolution NMR, HPLC, and LC-MS/MS could be applied for this purpose, and could be used to  
235 test predictions of the HBH. Omics approaches, including functional genomics, provide an  
236 avenue that could be applied in marine systems to measure the expression and activity of  
237 oxygenase enzymes involved in ODDOM metabolism, and to characterize of the responses of  
238 plankton cells and communities to suboxia.

239 The HBH has broader implications that could be explored with global data. It posits that rates of  
240 oxygen loss and DOM oxidation slow as DO approaches hypoxia, setting the upper bounds for  
241 the size of oceanic anoxic zones and organic carbon pools within. This can be evaluated in detail  
242 by modeling studies that test the sensitivity of model-data comparisons to changes in  
243 assumptions about microbial kinetic constants for oxygen.

244 **Alternatives to the HBH.** While we propose HBH to explain declines in oxygen frequency  
245 distributions at unexpected high values (Figs. 2 and S2) and the rarity of suboxia and anoxia  
246 across productive, low oxygen EBUS, alternate scenarios could explain this phenomenon. For  
247 example, consistent barriers to oxygen diffusion to the terminal oxidases of respiratory systems,  
248 or feedback mechanisms involving the production of sulfides and/or depletion of DO in  
249 microhabitats, or oxygen limitation of metazoan grazing, could play a role in suppressing  
250 respiration at low oxygen concentrations. Alternatively, there may be constraints on supply of

251 organic carbon or positive feedbacks on the resupply of DO by advection or diffusion as DO  
252 approaches hypoxia.

253 **Public interest and policy.** The relevance of this issue to public interests in ecosystem  
254 management could not be more profound. Ocean deoxygenation, the decline in ocean oxygen  
255 inventories, has emerged as a leading pathway for climate change impacts in the sea. This  
256 decline has been linked with expansion of hypoxic and anoxic zones. Oxygen deficient zones are  
257 hotspots of biogeochemical transformations whose growth can have profound impacts on marine  
258 biodiversity, vertical organic carbon flux, the sustainability of fisheries and feedbacks that  
259 govern ocean nitrogen budgets and flux of radiatively active N<sub>2</sub>O. The ability to accurately  
260 forecast such ecosystem changes is central for informing responsive climate change mitigation  
261 and adaptation policies. However, the disagreement between observations and the textbook  
262 understanding of microbial respiration raises fundamental questions about the mechanisms that  
263 underlie our conceptual and numerical models of the ocean dynamics as climate change  
264 intensifies. The HBH offers a testable framework for examining a potentially flawed  
265 fundamental principle that governs our thinking about OMZ formation. If this hypothesis is  
266 correct, it will open previously overlooked avenues of research at the intersection of oxygenase  
267 enzyme evolution, oxygenase-dependent metabolism in microbial communities, and OMZ  
268 dynamics.

269 **Conclusion.** If these ideas have the power to even partially explain the kinetics of ocean oxygen  
270 depletion, they could contribute to a better understanding of climate change impacts on ocean  
271 deoxygenation and DOM chemistry. The data in Fig. 1 show us that the HBH is founded on  
272 sound basic principles, but the impact of oxygenase “barrier” we describe is relative to many  
273 other processes, mentioned above, that can also slow respiration, most notably diffusion. Sorting

274 out the magnitude of catabolic oxygenase enzyme contributions to DOM oxidation, whether that  
275 number be large or small, will help us assess how the trajectories of aquatic systems  
276 experiencing oxygen declines are shaped by the fundamental biochemistry described in the HBH.

## 277 **MATERIAL AND METHODS**

278 **Data collection.** Scientific literature was mined for characterized oxygenase enzymes with  
279 published  $K_m$  values for dissolved oxygen for both individual enzyme assays as well as whole  
280 cell assays (Table S1). Metadata, including enzyme name and host scientific organism name,  
281 were extracted from each article. We used a combination of BRENDA enzyme database, uniprot  
282 protein database, and KEGG database searches to determine putative protein accessions, KEGG  
283 ortholog IDs, and EC numbers associated with the published enzyme data. Repeated entries for  
284 the same organism-protein pairs were included due to the various testing conditions per study.

285 Basin and global inventories of DO volumes were compiled from the World Ocean Atlas 2018  
286 (<https://www.ncei.noaa.gov/products/world-ocean-atlas>. Dissolved oxygen observations (5-  
287 400m) from CTD profiles were compiled from Chan et al. 2008, <https://www3.mbari.org/bog/>,  
288 and <https://www.calcofi.org/> for the northern (n=107,032 1950 to 2006), central (n=4,372 1997-  
289 2013), and southern (n=4,372 1997-2013) CCS, respectively.

290 **Respiration rate experiment.** Water samples were drawn from above and within the CCS OMZ  
291 (46 47.56°N, 125 11.83°W, 1000m station depth) and filled into 300ml borosilicate glass BOD  
292 bottles that each contained an oxygen optode dot (PreSens Precision Sensing GmbH). On filling,  
293 DO in a subset of samples initial [DO] were increased by allowing air to be entrained momen-  
294 tarily in the Niskin outflow tubing. Bottles were incubated in a ~6°C water bath in the dark. DO  
295 change over 48 was measured through the glass via detection of phase shift luminescence.

296

297 **Boxplot generation.** Km-DO values were split into two primary groups dependent upon general  
298 protein function, either respiratory oxidases or non-respiratory oxidases.  $K_m$ -DO values were  
299 also gathered for whole cells, whereby labile and semi-labile carbon sources were compared,  
300 mirroring the respiratory and non-respiratory individual enzyme assays. Plots were generated  
301 with the grouped Km-DO values using R v4.0.2 (23) and the ggplot2 (24). A linear mixed  
302 effects model was used to control for repeated  $O_2$  Km measurements from the same organism,  
303 with the formula  $\log(K_m) \sim \text{oxidase type} + (1 | \text{organism})$ . The model was fit using maximum  
304 likelihood, and the t-test to confirm significant difference of the coefficient for oxidase type was  
305 done using Satterthwaite's method for degrees of freedom (17). Log (natural) transformed values  
306 were used to approximate normality in the data. R code for this analysis can be found at github  
307 repo: <https://github.com/davised/HBH-2021>.

## 308 **ACKNOWLEDGEMENTS**

309 We thank the reviewers, John Coates and Dave Valentine, for their many useful comments. John  
310 Coates offered the important insight that intracellular competition with respiratory oxygenases  
311 could contribute to the inhibition of non-respiratory oxygenases. This work was funded by the  
312 National Science Foundation grant DEB-1639033, NOAA grant NA18NOS4780169, a SciRIS  
313 award from the Oregon State University College of Science, and a grant from Simons  
314 Foundation International. No authors declare any real or perceived financial conflicts of interests.

315 **REFERENCES (24/25)**

- 316 1. Levin LA. 2018. Manifestation, drivers, and emergence of open ocean deoxygenation.  
317 Annual Review of Marine Science, Vol 10 10:229-260.
- 318 2. Deutsch C, Brix H, Ito T, Frenzel H, Thompson L. 2011. Climate-forced variability of  
319 ocean hypoxia. Science 333:336-339.
- 320 3. Revsbech NP, Larsen LH, Gundersen J, Dalsgaard T, Ulloa O, Thamdrup B. 2009.  
321 Determination of ultra-low oxygen concentrations in oxygen minimum zones by the  
322 STOX sensor. Limnology and Oceanography-Methods 7:371-381.
- 323 4. Longmuir IS. 1954. Respiration rate of bacteria as a function of oxygen concentration.  
324 Biochem:81-87.
- 325 5. Zakem EJ, Follows MJ. 2017. A theoretical basis for a nanomolar critical oxygen  
326 concentration. Limnology and Oceanography 62:795-805.
- 327 6. Cavan EL, Trimmer M, Shelley F, Sanders R. 2017. Remineralization of particulate  
328 organic carbon in an ocean oxygen minimum zone. Nat Commun 8:14847.
- 329 7. Robinson C. 2019. Microbial Respiration, the Engine of Ocean Deoxygenation. Frontiers  
330 in Marine Science 5.
- 331 8. Stolper DA, Revsbech NP, Canfield DE. 2010. Aerobic growth at nanomolar oxygen  
332 concentrations. Proceedings of the National Academy of Sciences of the United States of  
333 America 107:18755-18760.
- 334 9. Keil RG, Neibauer JA, Biladeau C, van der Elst K, Devol AH. 2016. A multiproxy  
335 approach to understanding the "enhanced" flux of organic matter through the oxygen-  
336 deficient waters of the Arabian Sea. Biogeosciences 13:2077-2092.

- 337 10. Kalvelage T, Lavik G, Jensen MM, Revsbech NP, Loscher C, Schunck H, Desai DK,  
338 Hauss H, Kiko R, Holtappels M, LaRoche J, Schmitz RA, Graco MI, Kuypers MMM.  
339 2015. Aerobic microbial respiration In oceanic oxygen minimum zones. Plos One 10.
- 340 11. Sampou P, Kemp WM. 1994. Factors Regulating Plankton Community Respiration in  
341 Chesapeake Bay. Marine Ecology Progress Series 110:249-258.
- 342 12. Holtappels M, Tiano L, Kalvelage T, Lavik G, Revsbech NP, Kuypers MMM. 2014.  
343 Aquatic respiration rate measurements at low oxygen concentrations. Plos One 9.
- 344 13. Laufkotter C, John JG, Stock CA, Dunne JP. 2017. Temperature and oxygen dependence  
345 of the remineralization of organic matter. Global Biogeochemical Cycles 31:1038-1050.
- 346 14. DeVries T, Weber T. 2017. The export and fate of organic matter in the ocean: New  
347 constraints from combining satellite and oceanographic tracer observations. Global  
348 Biogeochemical Cycles 31:535-555.
- 349 15. Krooneman J, Wieringa EB, Moore ER, Gerritse J, Prins RA, Gottschal JC. 1996.  
350 Isolation of *Alcaligenes* sp. strain L6 at low oxygen concentrations and degradation of 3-  
351 chlorobenzoate via a pathway not involving (chloro)catechols. Appl Environ Microbiol  
352 62:2427-2434.
- 353 16. Leahy JG, Johnson GR, Olsen RH. 1997. Cross-regulation of toluene monooxygenases  
354 by the transcriptional activators TbmR and TbuT. Appl Environ Microbiol 63:3736-9.
- 355 17. Kuznetsova A, Brockhoff PB, Christensen RHB. 2017. lmerTest Package: Tests in Linear  
356 Mixed Effects Models. 2017 82:26.
- 357 18. Fox NK, Brenner SE, Chandonia JM. 2014. SCOPe: Structural Classification of Proteins-  
358 -extended, integrating SCOP and ASTRAL data and classification of new structures.  
359 Nucleic Acids Res 42:D304-309.



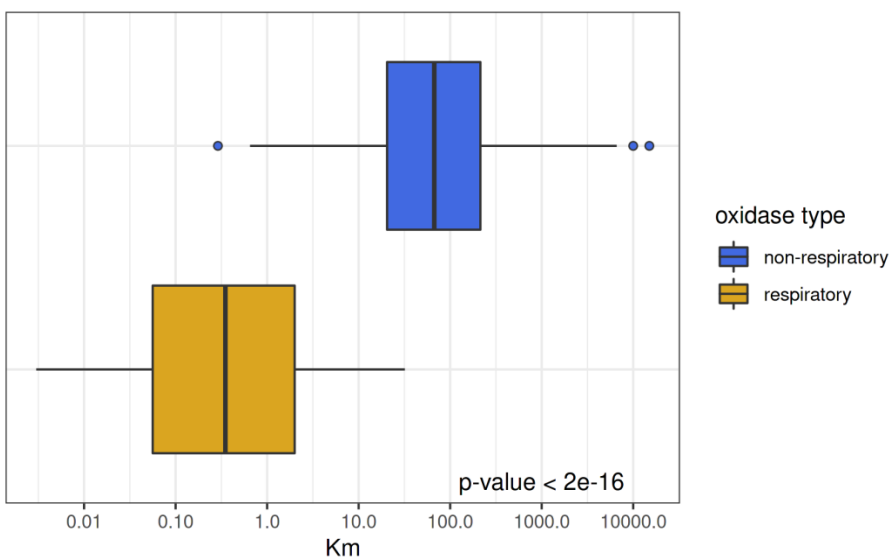
- 360 19. Floudas D, Binder M, Riley R, Barry K, Blanchette RA, Henrissat B, Martinez AT,  
361 Otilar R, Spatafora JW, Yadav JS, Aerts A, Benoit I, Boyd A, Carlson A, Copeland A,  
362 Coutinho PM, de Vries RP, Ferreira P, Findley K, Foster B, Gaskell J, Glotzer D,  
363 Gorecki P, Heitman J, Hesse C, Hori C, Igarashi K, Jurgens JA, Kallen N, Kersten P,  
364 Kohler A, Kues U, Kumar TK, Kuo A, LaButti K, Larrondo LF, Lindquist E, Ling A,  
365 Lombard V, Lucas S, Lundell T, Martin R, McLaughlin DJ, Morgenstern I, Morin E,  
366 Murat C, Nagy LG, Nolan M, Ohm RA, Patyshakuliyeva A, et al. 2012. The Paleozoic  
367 origin of enzymatic lignin decomposition reconstructed from 31 fungal genomes. *Science*  
368 336:1715-1719.
- 369 20. Huijbers MM, Montersino S, Westphal AH, Tischler D, van Berkel WJ. 2014. Flavin  
370 dependent monooxygenases. *Arch Biochem Biophys* 544:2-17.
- 371 21. Landry Z, Swan BK, Herndl GJ, Stepanauskas R, Giovannoni SJ. 2017. SAR202  
372 Genomes from the Dark Ocean Predict Pathways for the Oxidation of Recalcitrant  
373 Dissolved Organic Matter. *mBio* 8.
- 374 22. Kits KD, Klotz MG, Stein LY. 2015. Methane oxidation coupled to nitrate reduction  
375 under hypoxia by the Gammaproteobacterium *Methylomonas denitrificans*, sp nov type  
376 strain FJG1. *Environmental Microbiology* 17:3219-3232.
- 377 23. Team RC. 2020. R: A language and environment for statistical computing. R Foundation  
378 for Statistical Computing, Vienna, Austria <https://www.R-project.org/>.
- 379 24. Wickham H. 2016. *Elegant Graphics for Data Analysis*. Springer-Verlag New York.

380

381

382

383 **FIGURES**



384

385 **Figure 1.**  $K_m$  values are significantly smaller in respiratory oxidases compared to other

386 oxygenases.  $K_m$ -DO (dissolved oxygen) values for respiratory oxidases (yellow; n=109) and

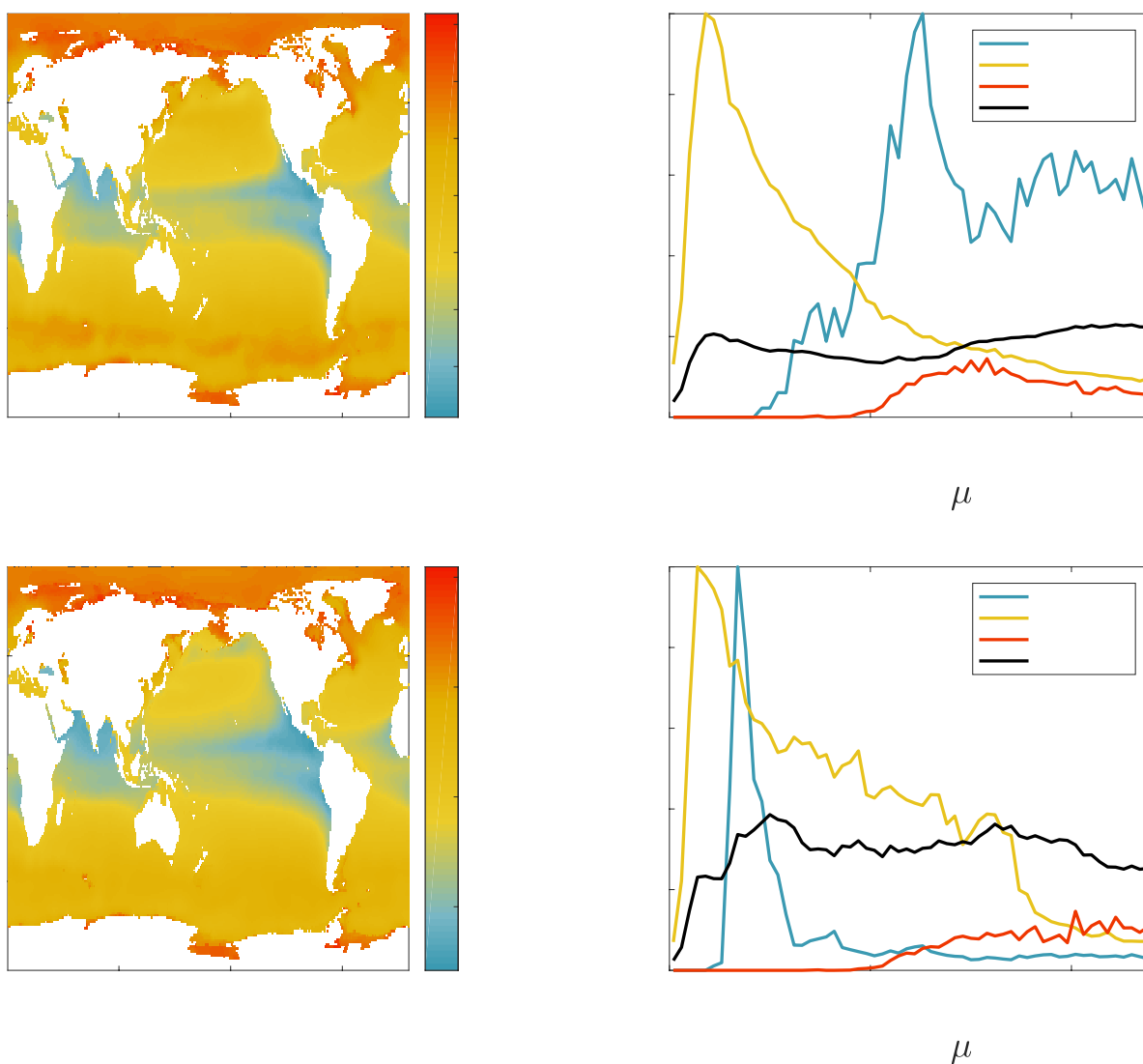
387 other oxygenases (blue; n=890) are depicted on a log<sub>10</sub> scale. The relatively high (e.g.  $10^1$   $\mu$ M)

388  $K_m$  values reported for oxidase enzymes indicate a potential bottleneck in the supply of electrons

389 from organic matter to respiration. The reported p-value is from a t-test using the Satterthwaite

390 approximations to degrees of freedom of a linear mixed model fit by maximum likelihood. Data

391 and citations can be found in Table S1.



392

393 **Figure 2.** Climatological DO concentrations and distribution of ocean volume across DO  
394 concentrations relationships for the California Current System (CCS), Eastern Tropical Pacific  
395 (EastTropPac), Eastern Tropical Atlantic (EastTropAtl) and global ocean. (A) 0-400 m,  
396 represents generally annual to decadal-scale processes, relative to ventilation and biomass  
397 formation by photosynthesis, (B) 0-1000 m, encompasses decadal to centennial-scale processes.

398

399

## 400 SUPPLEMENTAL MATERIALS

401 **Table S1.** Literature reports of  $K_m$  values for oxygenase enzymes and terminal respiratory  
402 oxidases used to construct Figs 1 and S1.

403

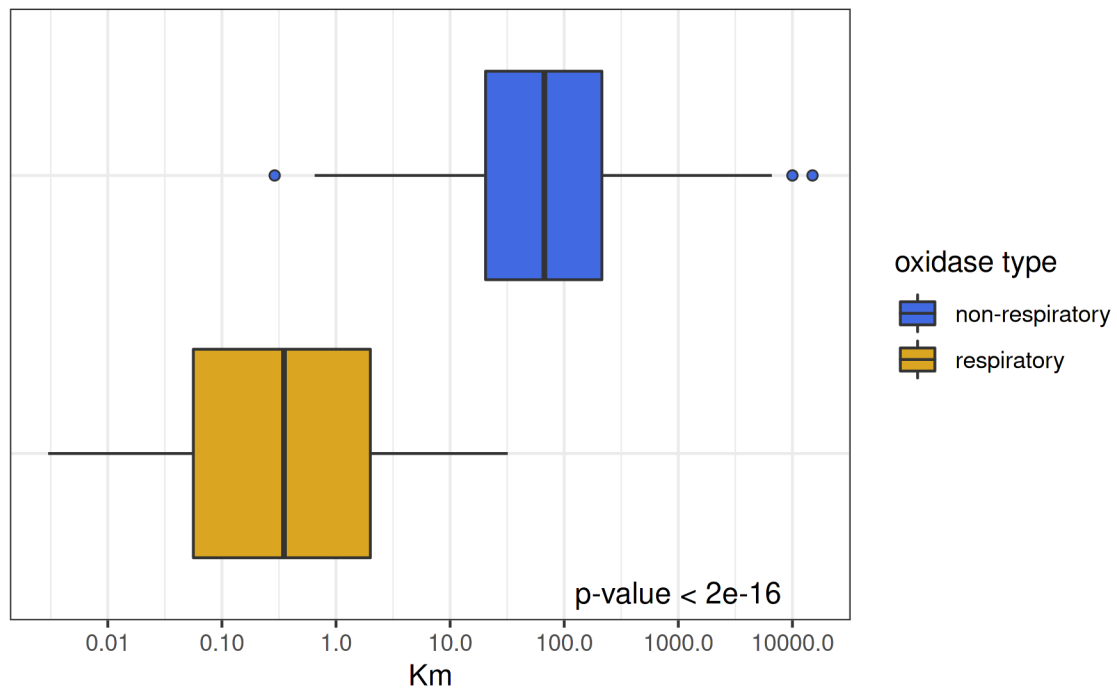
404 **Fig. S1.** Oxidase density plot. This plot illustrates the distribution of oxygenase  $K_m$  values  
405 reported in the literature for respiratory and non-respiratory oxidases (A) compared to whole cell  
406 assays including labile and semi-labile carbon sources (B).

407

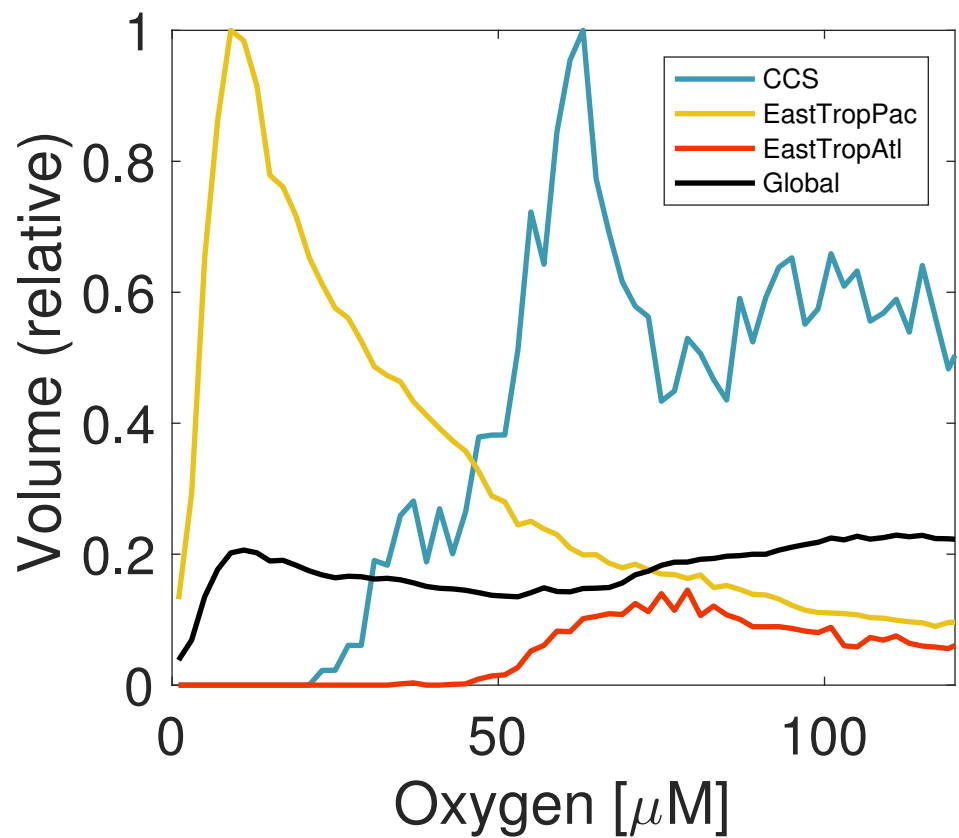
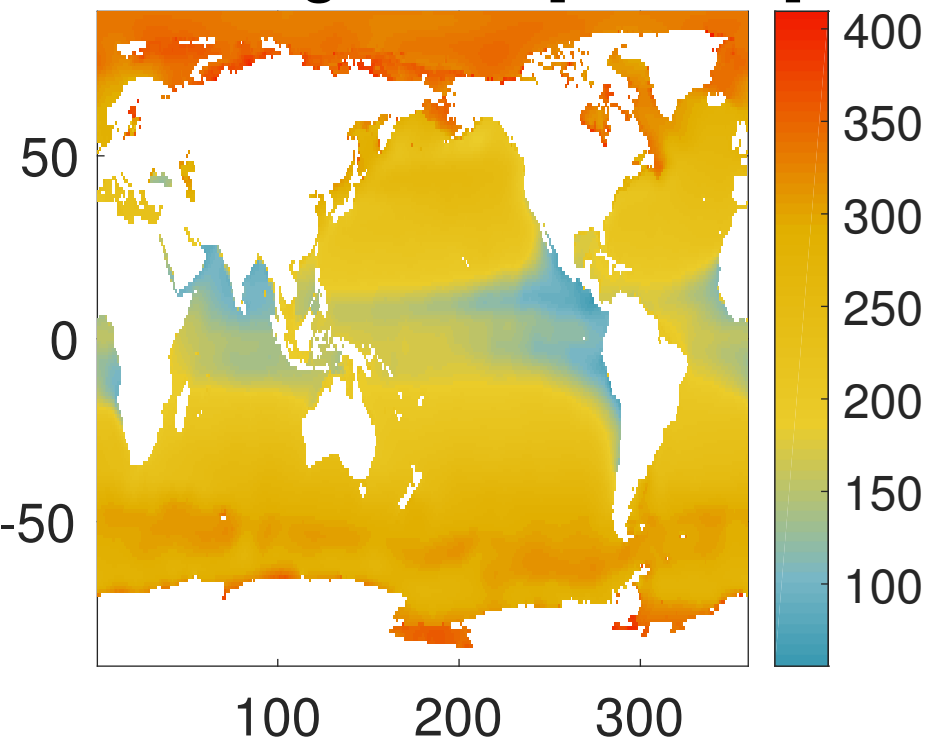
408 **Fig. S2.** Cumulative frequency distribution of DO observations from continental shelf depths (5-  
409 400 m, i.e. above the OMZ) for the northern (—), central (—), and southern (—) California  
410 Current System (CCS). Note the rarity of DO observations  $< 25 \mu\text{M}$  and an apparent hinge in the  
411 frequency of observations as DO increases beyond that concentration.

412 **Fig. S3.** Examples of respiration rates from field collected samples that exhibited non-saturating  
413 dynamics at 10's of  $\mu\text{M}$   $[\text{O}_2]$ . In each instance, respiration rates were assayed in samples where  
414  $[\text{O}_2]$  was manipulated independently. Data from the CCS were measured via  $\text{O}_2$  optode equipped  
415 glass bottles from water samples collected within the OMZ. Oxygen was increased by allowing  
416 air to be momentarily entrained as bottles were filled.

417



### Climatological O2 [0-400 m]



### Climatological O2 [0-1000 m]

